JACS
JOURNAL OF THE AMERICAN CHEMICAL SOCIETY

ARTICLE

pubs.acs.org/JACS

Competition between Li^+ and Mg^{2+} in Metalloproteins. Implications for Lithium Therapy

Todor Dudev*,† and Carmay Lim*,†,‡

†Institute of Biomedical Sciences, Academia Sinica, Taipei 115, Taiwan

‡Department of Chemistry, National Tsing Hua University, Hsinchu 300, Taiwan

Supporting Information

ABSTRACT: Lithium is used (in the form of soluble salts) to treat bipolar disorder and has been considered as a possible drug in treating chronic neurodegenerative diseases such as Alzheimer's, Parkinson's, and Huntington's diseases. One of the proposed mechanisms of Li^+ action involves a competition between the alien Li^+ and native Mg^{2+} for metal-binding sites and subsequent inhibition of key enzymes involved in specific neurotransmission pathways, but *not* vital Mg^{2+} proteins in the cell. This raises the following intriguing questions: Why does Li^+ replace Mg^{2+} only in enzymes involved in bipolar disorder, but not in Mg^{2+} proteins essential to cells? In general, what factors allow monovalent Li^+ to displace divalent Mg^{2+} in proteins? Specifically, how do the composition, overall charge, and solvent exposure of the metal-binding site as well as a metal-bound phosphate affect the selectivity of Li^+ over Mg^{2+}? Among the many possible factors, we show that the competition between Mg^{2+} and Li^+ depends on the net charge of the metal complex, which is determined by the numbers of metal cations and negatively charged ligands, as well as the relative solvent exposure of the metal cavity. The protein itself is found to select Mg^{2+} over the monovalent Li^+ by providing a solvent-inaccessible Mg^{2+}-binding site lined by negatively charged Asp/Glu, whereas the cell machinery was found to select Mg^{2+} among other competing divalent cations in the cellular fluids such as Ca^{2+} and Zn^{2+} by maintaining a high concentration ratio of Mg^{2+} to its biogenic competitor in various biological compartments. The calculations reveal why Li^+ replaces Mg^{2+} only in enzymes that are known targets of Li^+ therapy, but not in Mg^{2+} enzymes essential to cells, and also reveal features common to the former that differ from those in the latter proteins.

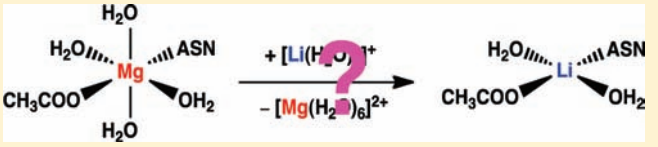

INTRODUCTION

Magnesium is one of the most versatile metal cofactors in cellular biochemistry, serving both structural and catalytic roles. It is employed by Nature to stabilize a variety of protein structures, nucleic acids, and biological membranes.[1−5] It also plays a pivotal role in a plethora of enzymatic processes that utilize/synthesize adenosine triphosphate (ATP) as well as in enzymes that regulate the biochemistry of nucleic acids such as restriction nucleases, ligases, and topoisomerases.[2] Furthermore, Mg^{2+}-dependent enzymes such as glycogen synthase kinase-3 (GSK-3), inositol monophosphatase (IMPase), inositol polyphosphate phosphatase, and G-proteins function as key components of multiple signaling pathways in living cells.[6−9]

Mg^{2+}, being a "hard" ion, prefers "hard" ligands of low polarizability, with the Asp/Glu carboxylate oxygen being the most preferred coordinating atom in proteins.[5,10−12] Mg-binding sites in the Protein Data Bank[13] (PDB) structures of Mg^{2+} enzymes generally contain one or more carboxylate ligands,[10] which bind Mg^{2+} predominantly via one carboxylate oxygen (monodentate) rather than both carboxylate oxygen atoms (bidentate).[5,14−16] Among the noncharged protein ligands coordinated to Mg^{2+}, the backbone carbonyl groups and the Asn/Gln side chains are the most common, followed by the Ser/Thr and His side chains.[10,12,17] Since Mg^{2+} is usually octahedrally coordinated, the rest of the metal's coordination sphere is occupied by water ligand(s) in the absence of other low-molecular-weight cofactors.

Studies on the competition between Mg^{2+} and other divalent cations (e.g., Ca^{2+} and Zn^{2+})[11,12,16,18−23] or trivalent cations (e.g., La^{3+} and Al^{3+})[12,20,24−27] for Mg^{2+}-binding sites indicate that Mg^{2+} proteins are not very specific for Mg^{2+}. In general, Ca^{2+} cannot compete with Mg^{2+} for a given Mg^{2+}-binding site in proteins due to its lower charge density and thus lower affinity for the respective protein ligands.[28,29] In some cases, however, Ca^{2+} may bind to the Mg^{2+}-binding pocket more tightly than Mg^{2+} if it coordinates to Asp/Glu via both carboxylate O atoms (bidentate mode)[21] or if it binds to an extra Asp/Glu side chain in the vicinity of the metal cavity, as in the case of *Escherichia coli* ribonuclease HI.[19] On the other hand, divalent transition metals that are better charge-acceptors than Mg^{2+} (e.g., Zn^{2+}) may dislodge Mg^{2+} from an enzyme active site and inhibit enzymatic activity.[11,18] Notably, mononuclear Mg^{2+}-binding sites are more vulnerable to Zn^{2+} substitution than their bi- and trinuclear counterparts.[12,20] Thus, it appears that it is not the protein itself that has evolved to select Mg^{2+} from other divalent cations in the cellular fluids. Rather, it is the cell machinery that regulates the metal ion binding/selectivity process by maintaining an

Received: March 4, 2011
Published: May 19, 2011

Table 1. Comparison between Computed and Experimental Free Energies for $[MgX] + [Li(H_2O)_4]^+ \rightarrow [LiY] + [Mg(H_2O)_6]^{2+}$ in Water, $\Delta G^{80}(Li^+ \rightarrow Mg^{2+})$

		$\Delta G^{80}(Li^+ \rightarrow Mg^{2+})$ (kcal/mol)		
[MgX]	[LiY]	expt[a]	calcd	error[b]
$[Mg(H_2O)_5(CH_3COO^-)]^+$	$[Li(H_2O)_3(CH_3COO^-)]^0$	0.8	1.3	0.5
$[Mg(H_2O)_4(C_2O_4^{2-})]^0$	$[Li(H_2O)_2\ (C_2O_4^{2-})]^-$	2.7	2.1	−0.6
$[Mg(H_2O)_2(NTA^{3-})]^{-c}$	$[Li(NTA^{3-})]^{2-c}$	4.1	4.1	0.0

[a] Calculated from the experimental stability constants of the respective Mg^{2+} and Li^+ complexes from ref 58. [b] Error = ΔG^{80}(calcd) − ΔG^{80}(expt). [c] NTA = nitrilotriacetic acid bound in a tetradentate fashion (including central N atom) to the metal.

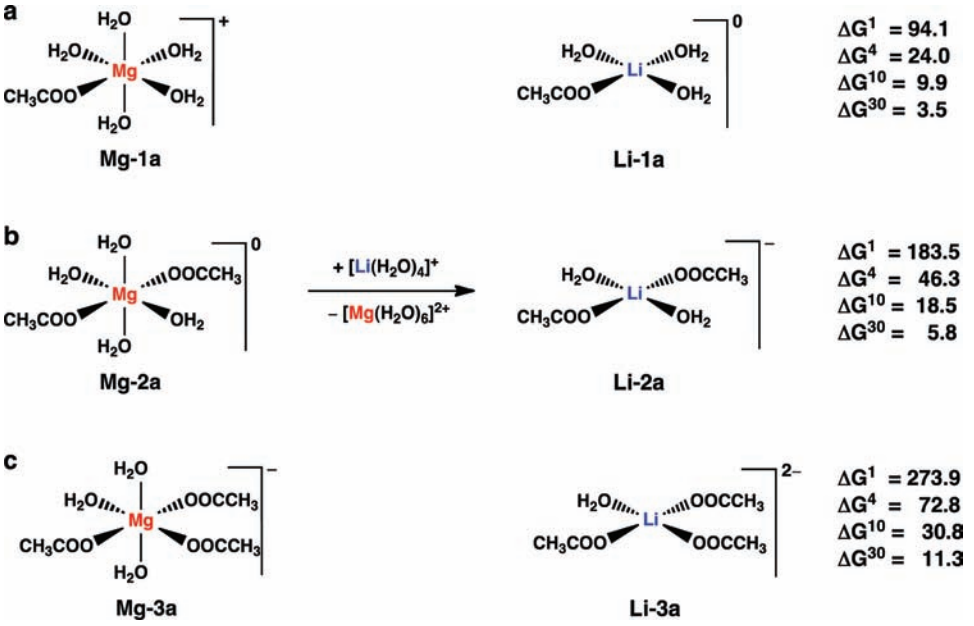

Figure 1. Free energies, ΔG^x (in kcal/mol), for replacing hexacoordinated Mg^{2+} with tetracoordinated Li^+ in a Mg-binding site lined by (a) one, (b) two, or (c) three carboxylates (modeled by CH_3COO^-).

appropriate concentration ratio of Mg^{2+} (10^{-3}–10^{-4} M[30]) to rival cations such as Ca^{2+} (10^{-7}–10^{-8} M[31]) and Zn^{2+} (~10^{-15} M[32]) in various biological compartments.[11,18,19] Apart from divalent cations, Mg^{2+}-binding sites are also ill protected against nonbiogenic trivalent metal cations. Theoretical studies show that Ln^{3+}/Al^{3+} can dislodge Mg^{2+} from the respective binding pocket(s).[12,20,24−27] Increasing the number of carboxylates and solvent inaccessibility of the metal-binding sites enhances the favorable electrostatic interactions with the trivalent cations, as compared with divalent Mg^{2+}, thus facilitating the substitution.[20,24,25] Thus, trivalent cations appear to exert their toxic effect by displacing the native metal cofactor from the protein active site, causing malfunction of the respective metalloproteins.[33,34]

Unlike the toxic trivalent cations, Li^+, a non-native metal ion with no known vital functions in humans and animals, is used (in the form of soluble salts) to treat bipolar disorder.[35] Recently, it has been considered as a possible drug in treating chronic neurodegenerative diseases such as Alzheimer's, Parkinson's, and Huntington's diseases.[35] Although the effect of Li^+ therapy has been known for decades, the mechanism of Li^+ action remains largely unknown. One of the leading hypotheses postulates a competition between the alien Li^+ and native Mg^{2+} for metal-binding sites and subsequent inhibition of key enzymes involved in specific neurotransmission pathways,[7,9,35] but *not* vital Mg^{2+} proteins in the cell. The rationale behind this hypothesis derives from the "diagonal relationship" between Li^+ and Mg^{2+}, reflecting the fact that most of the physicochemical properties of Li^+ are closer to those of Mg^{2+} (group IIA) than to those of its fellow alkali metals from group IA. For example, both Li^+ and Mg^{2+} are nonpolarizable "hard" cations with high charge density and strong affinity for "hard" O-containing ligands. They possess similar ionic radii (R_{ion}) for a given coordination number (CN): $R_{ion}(Li^+)$ = 0.59 Å and $R_{ion}(Mg^{2+})$ = 0.57 Å for a CN of 4, and $R_{ion}(Li^+)$ = 0.76 Å and $R_{ion}(Mg^{2+})$ = 0.72 Å for a CN of 6.[36] However, they have different ionic charge and significantly different hydration free energies (−123.5 kcal/mol for Li^+ and −455.5 kcal/mol for Mg^{2+}).[37] Interestingly, several experimental studies have shown that, *in vitro*, Li^+ can successfully compete with Mg^{2+} and bind to metal-binding sites in G-proteins,[38] GSK-3,[39,40] IMPase,[41] inositol polyphosphate phosphatase,[42] fructose-1,6-bisphosphatase,[43] and human erythrocyte membrane.[44] However, the detailed mechanism of the $Mg^{2+} \rightarrow Li^+$ substitution is not well understood, and several outstanding questions remain: (1) Clearly, for Li^+ to work as a drug, it cannot dislodge the native Mg^{2+} cofactor in essential Mg^{2+} proteins, so why does Li^+ replace Mg^{2+} only in certain enzymes involved in bipolar disorder (see

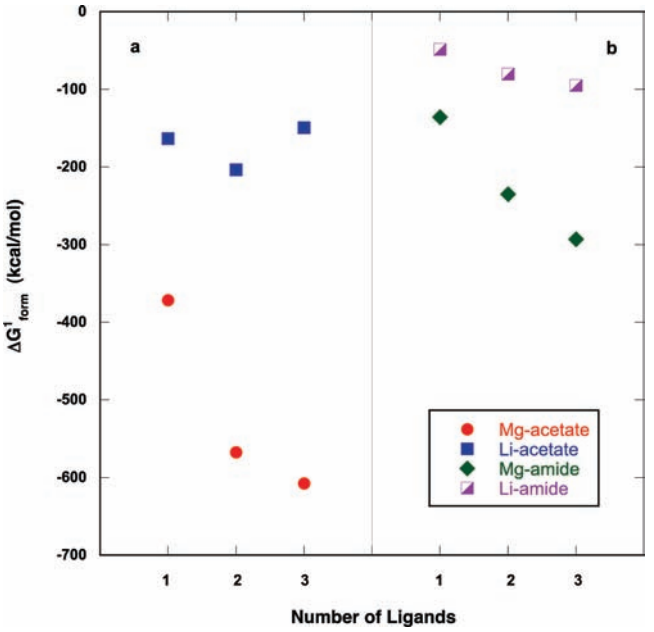

Figure 2. Plot of the gas-phase formation free energy for (a) $M^{q+} + n CH_3COO^- \rightarrow [M(CH_3COO)_n]^{q-n}$ ($M^{q+} = Mg^{2+}$, red circles; Li^+, blue squares) and (b) $M^{q+} + n CH_3CONHCH_3 \rightarrow [M(CH_3CONHCH_3)_n]^{q+}$ ($M = Mg^{2+}$, green diamonds; Li^+, purple semifilled squares) as a function of the number of metal-bound ligands, *n*.

above), but not in Mg^{2+} proteins essential to cells? (2) What factors dictate the competition between monovalent Li^+ and divalent Mg^{2+} in proteins? In particular, how do the composition, overall charge, and solvent exposure of the metal-binding site affect ion selectivity? (3) To what extent does a metal-bound phosphate at the active site influence the Li^+/Mg^{2+} competition?

To address the above questions, we systematically evaluated how the competition between Mg^{2+} and Li^+ in model metal-binding sites depends on (1) the number, chemical type, and charge of the protein ligating groups lining the binding pocket, (2) the number of Mg^{2+} cations in the enzyme active site, (3) the presence of a phosphate ligand bound to the active site metal, and (4) the solvent exposure of the binding pocket. Since our aim is to identify the key factors governing the selectivity of the native Mg^{2+} over the alien Li^+ in proteins in general, rather than a specific protein, the first-shell ligands and the metal cations were treated explicitly using density functional theory to account for electronic effects such as polarization of the participating entities and charge transfer from the ligands to the metal cation(s), whereas the rest of the protein was represented by a continuum dielectric constant varying from 4 to 30. Such an approach/model allows the strong electrostatic interactions between the two competing metal ions (Mg^{2+}/Li^+) and nearby metal ions and/or metal ligands to be treated as accurately as possible in computing the $Mg^{2+} \rightarrow Li^+$ exchange *free* energies (see Methods). The findings of this work help delineate the key determinants of selectivity for Mg^{2+} over Li^+ in Mg^{2+} proteins. They are consistent with available experimental data, and their implications in biology and Li^+ therapy are discussed.

METHODS

Models Used. The side chains of Asp^-/Glu^-, Asn/Gln, and peptide backbone group were modeled as acetate (CH_3COO^-), acetamide (CH_3CONH_2), and *N*-methylacetamide ($CH_3CONHCH_3$), respectively. The metal-bound monophosphate was represented by $H_2PO_4^-$, which is the dominant phosphate species at ambient pH.

Mono-, bi-, and trinuclear metal complexes were studied. In proteins, Mg^{2+} is mostly hexacoordinated,[45] as in aqueous solution.[46] Thus, Mg^{2+} complexes were modeled as MgL_6, $L_5Mg-L-MgL_5$, and $L_5Mg-L-MgL_4-L-MgL_5$ ($L = H_2O$, CH_3CONH_2, $CH_3CONHCH_3$, CH_3COO^-, or $H_2PO_4^-$). The most common coordination number of Li^+ is four.[47,48] Accordingly, its complexes were modeled as LiL_4, $L_3Li-L-MgL_5$, $L_5Mg-L-MgL_4-L-LiL_3$, and $L_3Li-L-MgL_4-L-MgL_5$ ($L = H_2O$, CH_3CONH_2, $CH_3CONHCH_3$, CH_3COO^-, or $H_2PO_4^-$). A monodentate carboxylate-binding mode to both metals was considered in accord with previous experimental and theoretical findings.[5,14−16]

Reaction Modeled. The competition between Mg^{2+} and Li^+ for the metal-binding site can be assessed by the free energy of the $Mg^{2+} \rightarrow Li^+$ exchange reaction,

$$[Mg^{2+}\text{-protein}] + [Li^+\text{-aq}] \rightarrow [Li^+\text{-protein}] + [Mg^{2+}\text{-aq}] \quad (1)$$

In eq 1, $[M^{q+}\text{-protein}]$ and $[M^{q+}\text{-aq}]$ represent the metal ion ($M^{q+} = Mg^{2+}$ or Li^+) bound to protein ligands and unbound in the vicinity of the binding cavity, respectively. The ion exchange free energy for eq 1 in an environment characterized by a dielectric constant $\varepsilon = x$ is given by

$$\Delta G^x = \Delta G^1 + \Delta G_{solv}{}^x([Li^+\text{-protein}]) + \Delta G_{solv}{}^x([Mg^{2+}\text{-aq}]) - \Delta G_{solv}{}^x([Mg^{2+}\text{-protein}]) - \Delta G_{solv}{}^x([Li^+\text{-aq}]) \quad (2)$$

where ΔG^1 is the gas-phase free energy for reaction 1, and $\Delta G_{solv}{}^x$ is the free energy for transferring a molecule in the gas phase to a medium characterized by dielectric constant *x*. The dielectric environment was assumed to be uniform for all participating entities, as the ion exchange was modeled to occur in the vicinity of the protein-binding site.

Gas-Phase Free Energy Calculations. Full geometry optimization for each metal complex was carried out using the Gaussian 03 program[49] with the B3-LYP functional and the 6-31+G(3d,p) basis set. This functional/basis set combination was chosen as it reproduces the experimental dipole moments of model ligands[50] and metal−ligand bond distances in metal complexes within experimental error: $R_{Li-O}{}^{calc} = 1.95$ Å and $R_{Li-O}{}^{exp} = 1.94 \pm 0.05$ Å in $[Li(H_2O)_4]^+$; $R_{Na-O}{}^{calc} = 2.75$ Å and $R_{Na-O}{}^{exp} = 2.77 \pm 0.07$ Å in [Na(18-crown-6-ether)]$^+$;[50] $R_{K-O}{}^{calc} = 2.82$ Å and $R_{K-O}{}^{exp} = 2.80 \pm 0.04$ Å in [K(18-crown-6-ether)]$^+$;[50] and $R_{Mg-O}{}^{calc} = 2.10$ Å and $R_{Mg-O}{}^{exp} = 2.07 \pm 0.03$ Å in $[Mg(H_2O)_6]^{2+}$.

For each fully optimized structure, vibrational frequencies were calculated to verify that the molecule was at the minimum of its potential energy surface. No imaginary frequency was found in any of the metal complexes. The electronic energy, E_{elec}, was evaluated at the same level of theory. The thermal energy, including the zero-point energy (E_T), work (PV), and entropy (S) corrections, was evaluated using standard statistical mechanical formulas,[51] where the B3-LYP/6-31+G(3d,p) frequencies were scaled by an empirical factor of 0.9613.[52] The differences ΔE_{elec}, ΔE_T, ΔPV, and ΔS between the products and reactants were used to compute the reaction free energy in the gas phase, ΔG^1, at room temperature, $T = 298.15$ K, according to

$$\Delta G^1 = \Delta E_{elec} + \Delta E_T + PV - T\Delta S \quad (3)$$

Solution Free Energy Calculations. The free energy for transferring a molecule in the gas phase to a medium characterized by dielectric constant $\varepsilon = x$, $\Delta G_{solv}{}^x$, was estimated by solving Poisson's equation using finite difference methods[53,54] with the Macroscopic Electrostatics with Atomic Detail (MEAD) program,[55] as described in previous works.[56] The effective solute radii were obtained by adjusting the CHARMM (version 22)[57] van der Waals radii to reproduce the experimental hydration free energies of Mg^{2+}, Li^+, CH_3COO^-,

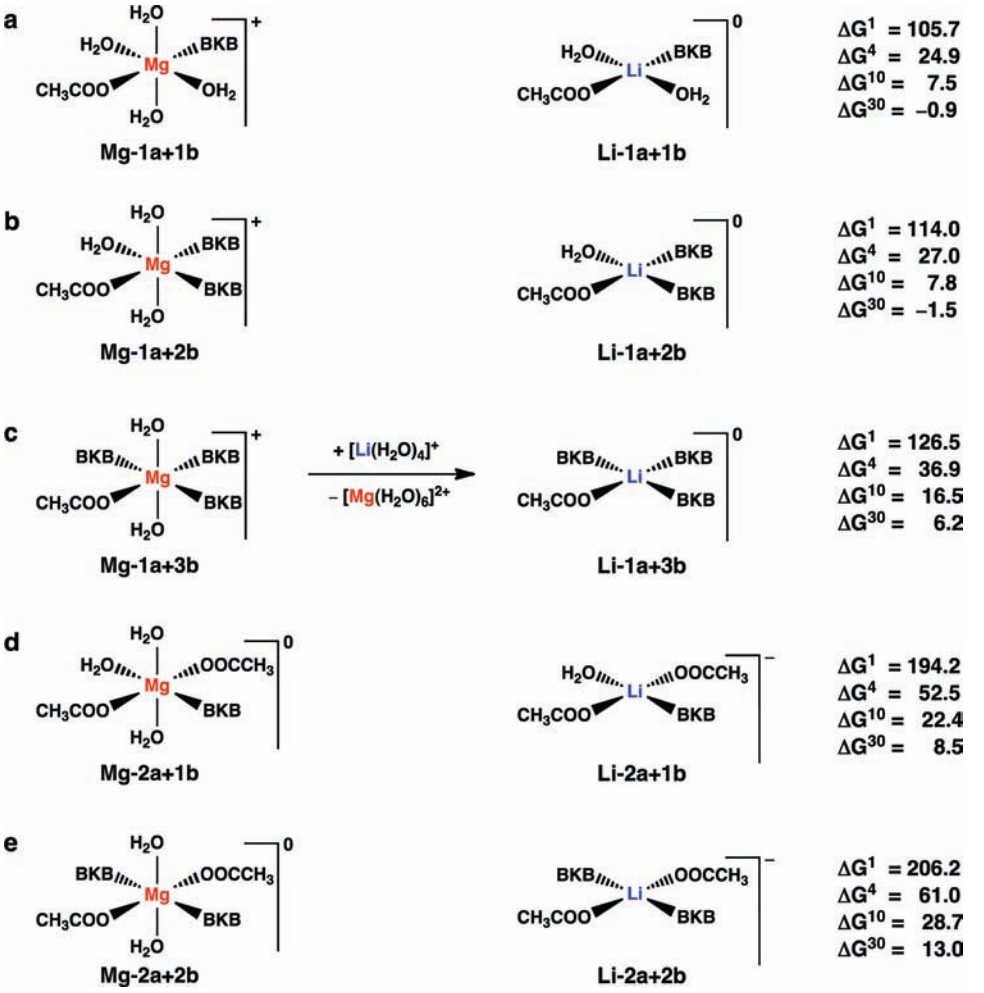

Figure 3. Free energies, ΔG^x (in kcal/mol), for replacing hexacoordinated Mg^{2+} with tetracoordinated Li^+ in a Mg-binding site lined by one or two carboxylates and one, two, or three backbone amide groups (modeled by $CH_3CONHCH_3$, denoted by BKB).

$H_2PO_4^-$, and $CH_3CONHCH_3$ (see Supporting Information, Table 1S) as well as the $Mg^{2+} \rightarrow Li^+$ free energies in one, two, and three carboxylate-containing complexes to within 1 kcal/mol (see Table 1). The resulting values (in Å) are $R_{Li} = 1.48$, $R_{Mg} = 1.50$, $R_C = 1.95$, $R_N = 1.75$, $R_P = 2.10$, $R_O(H_2O) = 1.84$, $R_O(O{=}C) = 1.72$, $R_O(COO{-}Li) = 1.56$, $R_O(COO{-}Mg) = 1.34$, $R_O(HO{-}P) = 1.60$, $R_O(OPO) = 1.50$, $R_H = 1.50$, $R_H(H_2O{-}Li) = 1.44$, $R_H(H_2O{-}Mg) = 1.125$, $R_H(P{-}OH) = 0.7$.

RESULTS

$Mg^{2+} \rightarrow Li^+$ Exchange in Mononuclear Sites Containing Carboxylates Only. Since functional Mg^{2+}-binding sites in enzymes have been found to contain at least one acidic residue (Asp/Glu) bound to Mg^{2+},[10,56] we modeled complexes with one, two, and three metal-bound acetates (denoted by "**a**"), with water ligands comprising the rest of the coordination shell. The free energies, ΔG^x, for replacing Mg^{2+} with Li^+ in these complexes in Figure 1 show that carboxylate-rich Mg^{2+}-binding sites appear immune to Li^+ substitution, regardless of whether they are buried or partially solvent exposed; notably, increasing the number of metal-bound carboxylates enhances the protection of these sites against Li^+ substitution. The gas-phase $Mg^{2+} \rightarrow Li^+$ free energies are highly positive and systematically increase with increasing number of carboxylates in the binding site: the ΔG^1 values are 94, 184, and 274 kcal/mol for complexes containing one (Figure 1a), two (Figure 1b), and three acetates (Figure 1c), respectively. This is because the negatively charged carboxylate(s) interact more favorably with divalent Mg^{2+} than monovalent Li^+, as shown by the formation free energies of these metal complexes in Figure 2a. Solvation, however, counterbalances the unfavorable electronic effects and results in much smaller ΔG^x ($x \geq 4$, Figure 1). This is because the solvation free energy gain of the outgoing Mg^{2+} dication outweighs the desolvation cost of the incoming Li^+ monocation. Moreover, for reactions b and c in Figure 1, the monoanionic **Li-2a** and dianionic **Li-3a** complexes are better solvated than the neutral **Mg-2a** and monoanionic **Mg-3a** bulkier complexes, respectively, which further enhances the net solvation free energy gain. Although the solvation contribution to the metal exchange free energy becomes more favorable with increasing solvent exposure of the binding site, the $Mg^{2+} \rightarrow Li^+$ free energy in a relatively solvent-exposed pocket remains positive ($\Delta G^{30} = 3.5$, 5.8, and 11.3 kcal/mol for reactions a, b and c in Figure 1, respectively).

$Mg^{2+} \rightarrow Li^+$ Exchange in Mononuclear Sites Containing Carboxylate and Backbone Ligands. In addition to the Asp/Glu side chains, the backbone peptide group (denoted by "**b**") is also frequently found bound to Mg^{2+} in proteins.[10,12,17] Therefore, it is of interest to study the $Mg^{2+} \rightarrow Li^+$ substitution in

dx.doi.org/10.1021/ja201985s |J. Am. Chem. Soc. 2011, 133, 9506–9515

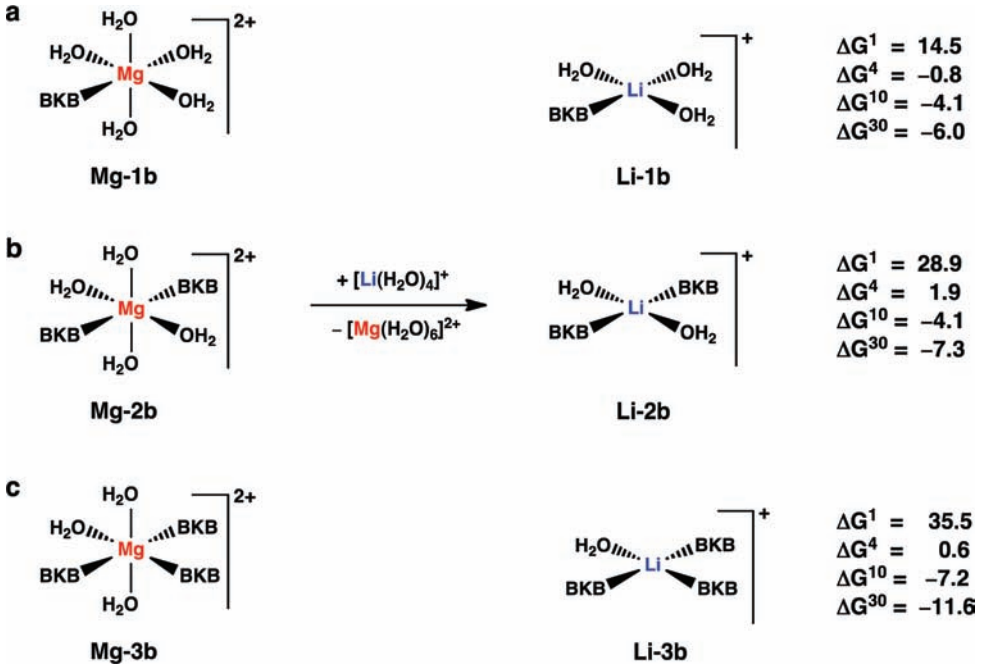

Figure 4. Free energies, ΔG^x (in kcal/mol), for replacing hexacoordinated Mg^{2+} with tetracoordinated Li^+ in a Mg-binding site lined by one, two, or three backbone amide groups.

binding sites comprising both Asp/Glu side chains (modeled by acetates) and backbone peptide groups (modeled by *N*-methylacetamide). The $Mg^{2+} \rightarrow Li^+$ free energies, ΔG^x, for these complexes in Figure 3 show that relatively buried Mg^{2+}-binding sites containing not only Asp/Glu but also backbone ligands appear immune to Li^+ substitution, like the Mg^{2+}–carboxylate complexes. Attaching backbone peptide groups to Mg^{2+} that is already bound to one or two acetates further increases the magnitude of the gas-phase free energies, as compared to the respective acetate-only complexes (compare the ΔG^1 values in Figures 1a and 3a–c or those in Figures 1b and 3d–e). For a given number of metal-bound carboxylates, the more backbone ligands bound to Mg^{2+}, the higher the $Mg^{2+} \rightarrow Li^+$ free energy in the gas phase; e.g., the ΔG^1 values in **Mg-1a+1b** (Figure 3a), **Mg-1a+2b** (Figure 3b), and **Mg-1a+3b** (Figure 3c) complexes are 106, 114, and 127 kcal/mol, respectively. This is because the larger dipole moment, polarizability, and stronger charge-donating ability of *N*-methylacetamide compared to water favor Mg^{2+} binding more than Li^+ binding (see Figure 2b). Solvation, again, significantly compensates for the unfavorable electronic effects and reduces the magnitude of the metal exchange free energy, which remains positive except for the ΔG^{30} values in reactions a (−0.9 kcal/mol) and b (−1.5 kcal/mol) in Figure 3. That the ΔG^x values decrease with increasing dielectric constant x suggests the possibility of Li^+ displacing Mg^{2+} bound to a carboxylate and one or two backbone ligands if the binding site were sufficiently exposed to solvent.

$Mg^{2+} \rightarrow Li^+$ Exchange in Mononuclear Sites Containing Backbones Only. Since the results in Figures 1 and 3 show that *decreasing* the number of metal-bound carboxylates lowers the $Mg^{2+} \rightarrow Li^+$ free energy, thus increasing the vulnerability of a Mg^{2+}-binding site toward Li^+ substitution, would a hypothetical binding site lacking negatively charged acidic residues be susceptible to Li^+ substitution? To answer this question, we modeled Mg^{2+} and Li^+ complexes with one, two, and three *N*-methylacetamides with the corresponding numbers of water molecules and evaluated the $Mg^{2+} \rightarrow Li^+$ free energies. The results in Figure 4 suggest that if Mg^{2+}–binding sites were comprised of only neutral protein ligands and not deeply buried, they would be prone to Li^+ substitution. Although the gas-phase free energies are positive and increase with increasing number of backbone ligands, they are much smaller than the respective free energies for complexes containing the same number of acetates: the ΔG^1 values in Figure 4 range from 15 to 36 kcal/mol, whereas those in Figure 1 range from 94 to 274 kcal/mol. This is because the metal cation has weaker electrostatic interactions with the neutral peptide backbone than with the negatively charged carboxylate, as evidenced by the more favorable formation free energies of the Mg^{2+}/Li^+–carboxylate complexes in Figure 2a compared with those of the respective Mg^{2+}/Li^+–backbone complexes in Figure 2b. Hence, the relatively small ΔG^1 for the carboxylate-empty binding sites are easily overcome by the net favorable solvation of the products relative to the reactants, thus yielding negative free energies for partially solvent-exposed ($\varepsilon \geq 10$) metal-binding sites.

$Mg^{2+} \rightarrow Li^+$ Exchange in Model GSK-3β Sites. Glycogen synthase kinase 3β (GSK-3β), a key Mg^{2+} enzyme involved in a variety of metabolic, signaling, and apoptotic mechanisms in the cell, is a potential therapeutic target of Li^+ in treating bipolar disorder and, possibly, Alzheimer's disease. There is an increasing body of experimental data suggesting that Li^+ exerts its therapeutic effect mainly by competitively dislodging Mg^{2+} from its binding site(s), thus inhibiting the GSK-3β phosphorylation activity in specific neurotransmission pathways in the brain.[39,40,59,60] However, the detailed mechanism of this process is not well understood. Even the composition of the metal-binding site is a subject of controversy: The 2.1 Å X-ray structure of GSK-3β with ADP (PDB entry 1j1c)[61] reveals a *mononuclear* Mg^{2+}-binding site located in a solvent-accessible cleft, lined with an aspartate (D200) and an

dx.doi.org/10.1021/ja201985s |*J. Am. Chem. Soc.* 2011, 133, 9506–9515

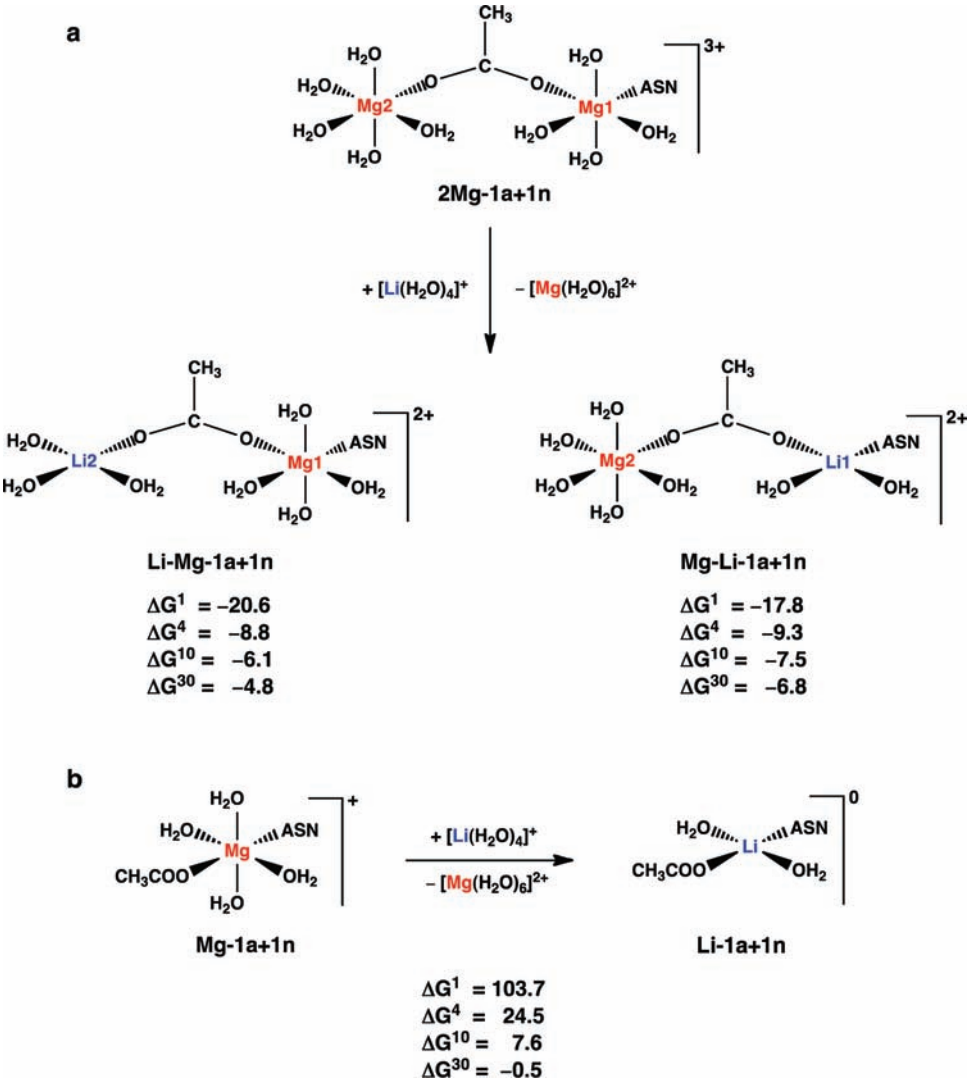

Figure 5. Free energies, ΔG^x (in kcal/mol), for replacing Mg^{2+} in site 1 or 2 with Li^+ in a model GSK-3β (a) binuclear or (b) mononuclear binding site lined by a carboxylate and Asn, modeled by CH_3CONH_2.

asparagine (N186). On the other hand, the 2.4 Å X-ray structure of GSK-3β with a nonhydrolyzable ATP analogue, adenyl imidodiphosphate (PDB entry 1pyx),[62] shows a *binuclear* Mg^{2+}-binding site with the same two ligands (D200 and N186) bound to Mg^{2+}, but with D200 additionally bound to a second Mg^{2+}. Therefore, both mononuclear and binuclear metal-binding sites in the absence of ATP analogues were modeled, and the $Mg^{2+} \rightarrow Li^+$ ΔG^x (x = 1−30) free energies for these sites were computed.

The results in Figure 5 indicate that the *binuclear* Mg^{2+}-binding site (**2Mg-1a+1n**, Figure 5a), lined by D200 and N186, is more vulnerable to Li^+ attack than the respective *mononuclear* binding site (**Mg-1a+1n**, Figure 5b), which would not be prone to $Mg^{2+} \rightarrow Li^+$ substitution unless it were solvent exposed. In the *binuclear* **2Mg-1a+1n** complex, replacing either of the Mg^{2+} cations by Li^+ is *favorable* in a buried or partially solvent-exposed site (Figure 5a, negative ΔG^x, x = 1−30). In the *mononuclear* **Mg-1a+1n** complex, replacing Mg^{2+} by Li^+ is unfavorable in relatively buried sites (Figure 5b, positive ΔG^x, $x \leq 10$) but not in solvent-exposed sites (with a dielectric constant $x > 30$). Note that the *N*-methylacetamide in the **Mg-1a+1b** complex (Figure 3a) is replaced by acetamide in the **Mg-1a+1n** complex (Figure 5b); hence, their structures and $Mg^{2+} \rightarrow Li^+$ free energies are similar.

To rationalize why the binuclear Mg^{2+}-binding site exhibits negative gas-phase ΔG^1 free energies (Figure 5a), whereas the mononuclear Mg^{2+}-binding sites possess positive ΔG^1 values (Figures 1, 3, 4, and 5b), the ΔG^1 values were plotted against the overall charge of the Mg^{2+} complex (Figure 6, red circles). The results show that the ΔG^1 values decrease with increasing positive net charge, Q, of the Mg^{2+} complex. The ΔG^1 decreases from a maximum of 274 kcal/mol for monoanionic complexes to 206−184, 127−94, and 36−15 kcal/mol for complexes with a net charge 0, 1+, and 2+, respectively. It becomes negative, −18 to −21 kcal/mol, for the binuclear Mg^{2+} complex with a net charge of 3+. Generally, Mg^{2+}-binding sites with increased positive charge density are more prone to $Mg^{2+} \rightarrow Li^+$ exchange in the condensed phase as well (Figure 6, blue squares), although the decrease in ΔG^x with increasing Q is much more gradual than that in the gas phase.

$Mg^{2+} \rightarrow Li^+$ Exchange in Model IMPase Polynuclear Sites. IMPase, a key trinuclear Mg^{2+} enzyme of the phosphatidylinositol signaling pathway, is another putative target for Li^+ therapy.[63−66]

dx.doi.org/10.1021/ja201985s |*J. Am. Chem. Soc.* 2011, 133, 9506–9515

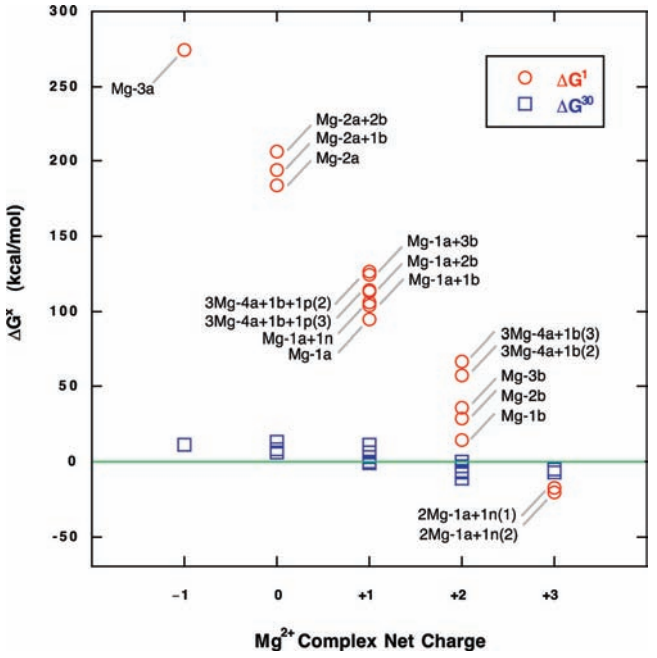

Figure 6. Plot of the $Mg^{2+} \rightarrow Li^{+}$ exchange free energies in the gas phase (red circles) and in a protein cavity characterized by $\varepsilon = 30$ (blue squares) as a function of the net charge of the Mg^{2+} complex.

The 1.4 Å X-ray structure of bovine IMPase (PDB entry 2bji) shows three Mg^{2+}-binding sites in a hydrophilic pocket near the enzyme's surface,[65] with Mg^{2+} at site 1 (Mg-1) coordinated to the E70 and D90 side chains and the I92 backbone, Mg^{2+} at site 2 (Mg-2) bound to the D90, D93, and D220 side chains, and Mg^{2+} at site 3 (Mg-3) ligated to a single protein ligand, E70. The D90 carboxylate bridges the Mg^{2+} ions at sites 1 and 2, while the E70 carboxylate bridges the Mg^{2+} ions at sites 1 and 3. Water molecules complete the octahedral coordination of each Mg^{2+} ion. Thus, the three Mg^{2+} are altogether bound to four carboxylates and one peptide backbone, and the corresponding model **3Mg-4a+1b** complex is depicted in Figure 7. Since the binding of Mg^{2+} to site 2 or 3 has been found to be much weaker than that to site 1,[65] we computed the $Mg^{2+} \rightarrow Li^{+}$ free energies at sites 2 and 3. The results in Figure 7 indicate that the dicationic **3Mg-4a+1b** complex is vulnerable to Li^{+} substitution, if the binding sites were relatively solvent exposed. The metal exchange free energies generally follow the dependency on the overall charge in Figure 6 (see above): the $Mg^{2+} \rightarrow Li^{+}$ ΔG^{1} values at sites 2 and 3 fall within the range of values for Mg^{2+} complexes with a net charge of 2+ (Figure 6). In the absence of substrate or reaction product, the $Mg^{2+} \rightarrow Li^{+}$ ΔG^{x} values for the dicationic **3Mg-4a+1b** complex are positive (unfavorable) when $x < 30$, but become negative when $x \geq 30$ (e.g., $\Delta G^{30} = -2.8$ kcal/mol at site 2). The calculations predict that the two binding sites have different affinity for Li^{+}, with site 2 being the more vulnerable to Li^{+} substitution, in line with a modeling study.[65]

Effect of a Metal-Bound Phosphate on the $Mg^{2+} \rightarrow Li^{+}$ Exchange. Since Li^{+} is thought to bind not only the free enzyme but also the Mg^{2+}–IMPase ternary complex, it is of interest to know whether a metal-bound phosphate favors/disfavors the $Mg^{2+} \rightarrow Li^{+}$ exchange. The model of the phosphate bound to IMPase trinuclear site was based on the 1.90 Å X-ray structure of yeast Hal2p PAPase-3Mg^{2+}-AMP-phosphate product complex,[65,67] in which the phosphate is bound to all three Mg^{2+} ions, as shown in Figure 8 (**3Mg-4a+1b+1p**). Since Li^{+} has been proposed to bind at site 2 or 3,[65] we computed the $Mg^{2+} \rightarrow Li^{+}$ free energies at these two sites. The results in Figure 8 show that binding of the negatively charged phosphate group to the trinuclear site disfavors $Mg^{2+} \rightarrow Li^{+}$ exchange regardless of the site of attack and its solvent exposure. The $Mg^{2+} \rightarrow Li^{+}$ free energies for the monocationic **3Mg-4a+1b+1p** are unfavorable compared with those of the dicationic **3Mg-4a+1b** complex (compare ΔG^{x} in Figures 8 and 7).

DISCUSSION

Factors Governing the Selectivity of Mg^{2+} over Li^{+} in Magnesium Proteins. In previous works,[11,18,19] the cell machinery was found to select Mg^{2+} among other competing dications in the cellular fluids such as Ca^{2+} and Zn^{2+} by maintaining a high concentration ratio of Mg^{2+} to its biogenic competitor in various biological compartments (see Introduction). In this work, the protein itself is generally found to select Mg^{2+} over the monovalent Li^{+} by providing a solvent-inaccessible Mg^{2+}-binding site lined by negatively charged Asp/Glu, although exceptions occur allowing Li^{+} to replace Mg^{2+}. The key properties of Mg^{2+}-binding sites that enable selective binding of Mg^{2+} over Li^{+} and vice versa are delineated below.

1. Complex Net Charge. The calculations herein reveal that the net charge of the metal complex, which is determined by the numbers of metal cations and acidic ligands, dictates the outcome of the Mg^{2+} vs Li^{+} competition. In a deeply buried cavity that enhances the charge–charge and charge–dipole interactions between the metal cation and protein ligands, increasing the number of carboxylates relative to that of the metal cations favors Mg^{2+} over Li^{+} because the dicationic Mg^{2+} has stronger interaction energies with negatively charged carboxylates and can tolerate more Asp/Glu ligands in its vicinity than monocationic Li^{+} (see Figure 2a).[56] In fact, as the net charge of the metal complex increases, the gas-phase $Mg^{2+} \rightarrow Li^{+}$ free energy decreases linearly, as evidenced by a Pearson's correlation coefficient of 0.983 (see Figure 6). On the other hand, Li^{+} may replace Mg^{2+} in a metal complex with net high positive charge, e.g., tricationic **2Mg-1a+1n** (Figure 5a), in a buried cavity since this reduces the net positive charge in the buried site.

2. Chemical Type of the Metal Ligand. The selectivity of Mg^{2+} over Li^{+} is determined not only by the metal ligand's charge but also by its size. Negatively charged metal ligands such as carboxylates and phosphates play a crucial role in selecting Mg^{2+} over Li^{+}. Notably, $H_2PO_4^{-}$ binds to Mg^{2+} and Li^{+} with the same relative affinity as acetate, as evidenced by the formation free energies, ΔG^{form}, for $M^{q+} + H_2PO_4^{-} \rightarrow [M(H_2PO_4)]^{q-1}$: $\Delta G^{form}[Mg(H_2PO_4)] - \Delta G^{form}[Li(H_2PO_4)] = -208.0$ kcal/mol, while $\Delta G^{form}[Mg(CH_3COO)] - \Delta G^{form}[Li(CH_3COO)] = -208.3$ kcal/mol. Thus, ligation of $H_2PO_4^{-}$ to Mg^{2+} has an effect similar to that of an extra carboxylate; viz., it inhibits $Mg^{2+} \rightarrow Li^{+}$ exchange (see Figure 8).

On the other hand, neutral metal ligands such as Asn/Gln and backbone amide groups play a dual role in the Mg^{2+}/Li^{+} selectivity process. Like the negatively charged carboxylate and phosphate ligands, the neutral amide ligands also disfavor substitution of Mg^{2+} by Li^{+} in the gas phase (Figures 3, 4 and 5b), but to a lesser extent. Compared to water, however, the bulkier amide increases the effective radius of the Mg^{2+} complex, which reduces the solvation free energy of the Mg^{2+} complex. This effect is especially significant for the smaller, charged complexes such as **Mg-1a+1b**, **Mg-1a+1n**, and **Mg-1a+2b**, where the decreased desolvation penalty of these

dx.doi.org/10.1021/ja201985s |J. Am. Chem. Soc. 2011, 133, 9506–9515

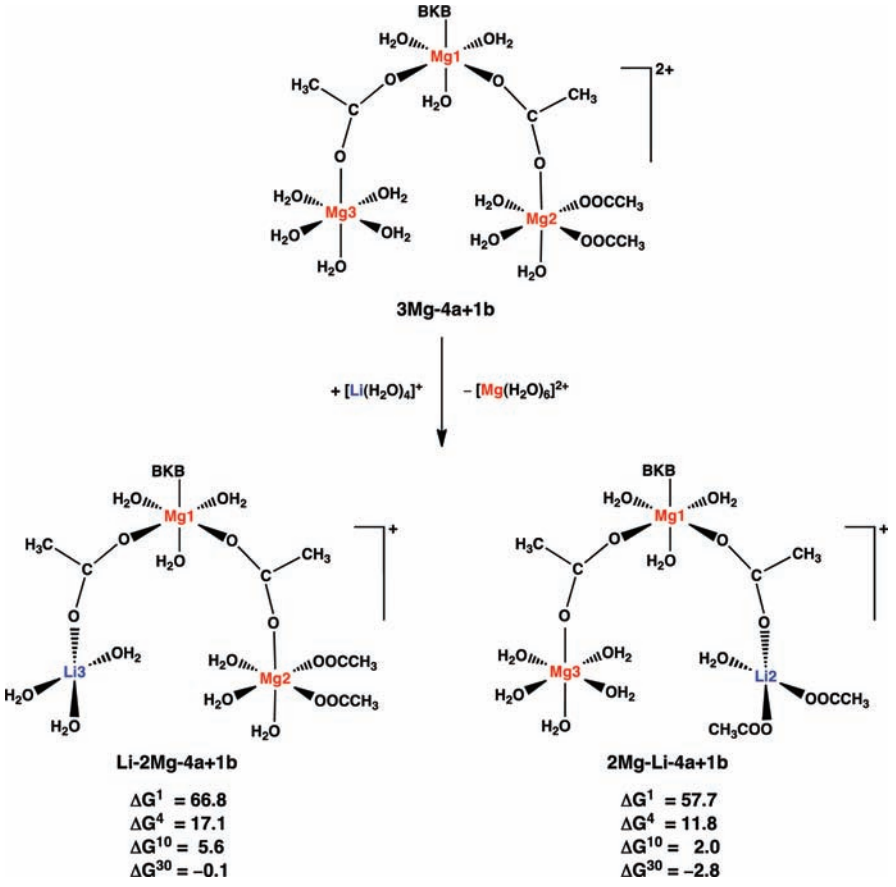

Figure 7. Free energies, ΔG^x (in kcal/mol), for replacing Mg^{2+} in site 2 or 3 with Li^+ in a model IMPase trinuclear binding site lined by four carboxylates and one backbone amide.

complexes relative to **Mg-1a** may overcome the unfavorable gas-phase electronic effects and yield negative $Mg^{2+} \rightarrow Li^+$ free energies in solvent-exposed binding sites (Figures 3a,b and 5b).

3. Solvent Exposure of the Binding Site. The relative solvent exposure of the metal cavity is another key determinant of the metal selectivity: For Mg^{2+} complexes with a net charge ≤ 2, increasing the solvent accessibility (i.e., ε) of the binding site decreases the $Mg^{2+} \rightarrow Li^+$ free energy mainly because the favorable solvation of the outgoing divalent Mg^{2+} outweighs the relatively small desolvation penalty of the incoming monovalent Li^+. However, this trend is reversed for Mg^{2+} complexes with a net charge of 3+ (Figure 5a), where the $Mg^{2+} \rightarrow Li^+$ free energy becomes less favorable with increasing solvent accessibility of the site, as the solvation of the dicationic **Li-Mg-1a+1n/Mg-Li-1a+1n** product complex cannot compensate the desolvation cost of the tricationic **2Mg-1a+1n** reactant complex.

Biological Implications. The calculations suggest that amide ligands alone cannot protect the Mg^{2+}-binding site from Li^+ (Figure 4) attack. This is consistent with the empirical finding that all functional Mg^{2+}-binding sites in enzymes found in a PDB survey contain at least one Asp or Glu ligand.[10] The results obtained imply that solvent-exposed Mg^{2+} sites lacking carboxylate ligands in enzymes may not be functional. Such sites would not have survived during cell evolution, mostly because of the poor selectivity for Mg^{2+} over monovalent metal ions.

Implications for the Mechanism of Li^+ Therapy. The calculations herein also suggest that in the GSK-3β enzyme, Li^+ can displace Mg^{2+} from a fully/partially buried binuclear site (Figure 5a, negative ΔG^x, $x \leq 30$) or a solvent-exposed mononuclear site (Figure 5b, negative ΔG^x, $x \gg 30$). This finding is consistent with experimental[39,40,59] studies showing that Li^+ inhibits GSK-3 isoforms by dislodging Mg^{2+} from the metal-binding site. It is also consistent with ONIOM calculations and MD simulations of the GSK-3β enzyme suggesting how Li^+ may inhibit enzymatic activity (by disrupting the in-line phosphoryl transfer of ATP).[68,69] Notably, our calculations identify the key factors allowing Li^+ to displace Mg^{2+}, viz., (i) low negative charge density (only D200) and (ii) a bulky amide metal ligand (N186) in both mono- and binuclear Mg^{2+}-binding sites, and (iii) a relatively solvent-accessible cleft in the case of a mononuclear binding site.

In addition to the GSK-3β enzyme, the calculations suggest that Li^+ can displace Mg^{2+} from its partially solvent-exposed binding site in free IMPase (Figure 7, negative ΔG^{30}). This finding appears consistent with the experimental observations that 0.5−1.5 mM Li^+ inhibits IMPase.[41,70,71] The calculations also expose the key factors favoring the $Mg^{2+} \rightarrow Li^+$ substitution in free IMPase, viz., the high positive charge (2+) and solvent exposure of the native trinuclear binding site.

Importantly, the calculations shed light on the intriguing question of why Li^+ replaces Mg^{2+} only in certain enzymes that are known targets of Li^+ therapy, but not in Mg^{2+} enzymes essential to cells, and reveal features common to the former that differ from those in the latter proteins. Enzymes that are targets of Li^+ therapy have Mg^{2+}-binding sites with high positive charge density, a few bulky ligands, and high solvent exposure for dicationic complexes but low solvent exposure for tricationic complexes. These characteristic

dx.doi.org/10.1021/ja201985s |*J. Am. Chem. Soc.* 2011, 133, 9506–9515

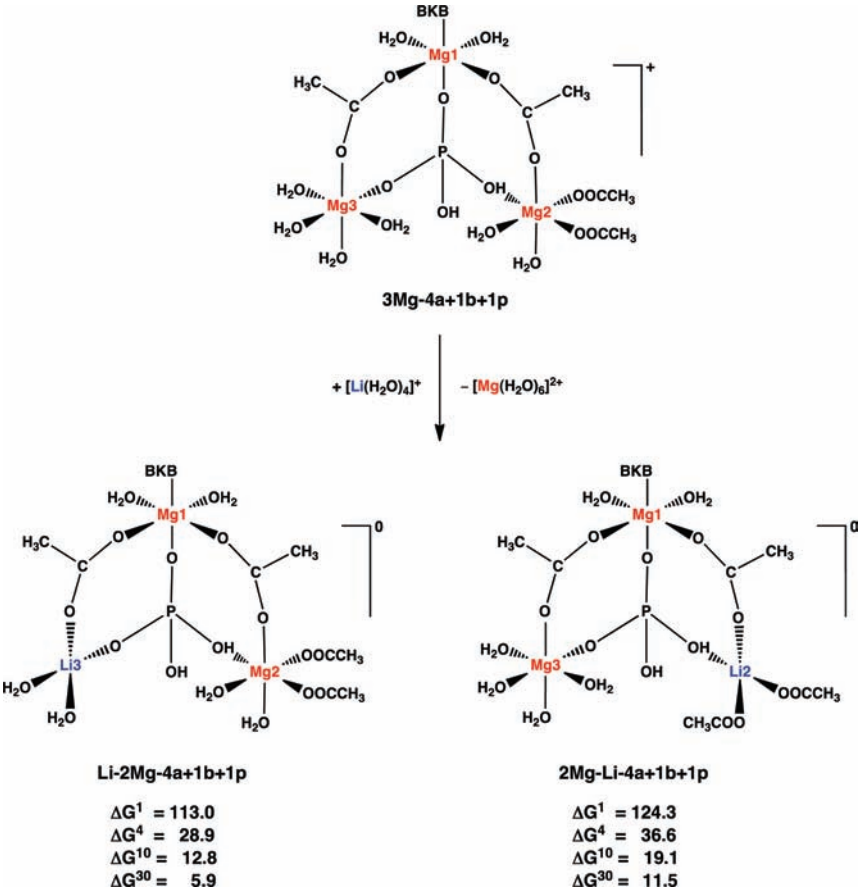

Figure 8. Free energies, ΔG^x (in kcal/mol), for replacing phosphate-bound Mg^{2+} in site 2 or 3 with Li^+ in a model IMPase trinuclear binding site lined by four carboxylates and one backbone amide.

features may provide guidelines to identify other enzymes that could be inhibited by Li^+. On the other hand, essential Mg^{2+} enzymes are known to have functional Mg^{2+}-binding sites containing at least one acidic residue and are deeply/partially buried.[10] Such sites containing neutral or anionic Mg^{2+} complexes are predicted to be protected against Li^+ attack (Figures 1 and 3, positive ΔG^x, $x \leq 10$). Binding of a negatively charged substrate group such as phosphate/polyphosphate to Mg^{2+} further protects such sites from Li^+ invasion (structure **3Mg-4a+1b+1p** in Figure 8).

■ ASSOCIATED CONTENT

Supporting Information. Complete refs 13 and 49 and Supporting Table S1. This material is available free of charge via the Internet at http://pubs.acs.org.

■ AUTHOR INFORMATION

Corresponding Author
carmay@gate.sinica.edu.tw; todor@ibms.sinica.edu.tw

■ ACKNOWLEDGMENT

Supported by Academia Sinica and the NSC (contract no. 95-2113-M-001-001).

■ REFERENCES

(1) Nordlund, P.; Sjoberg, B. M.; Eklund, H. *Nature* **1990**, *345*, 593.
(2) Cowan, J. A. *Biological Chemistry of Magnesium*; VCH: New York, 1995.
(3) Prasad, G. S.; Stura, E. A.; McRee, D. E.; Laco, G. S.; Hasselkus-Light, C.; Elder, J. H.; Stout, C. D. *Protein Sci.* **1996**, *5*, 2429.
(4) Dutzler, R.; Wang, Y. F.; Rizkallah, P.; Rosenbusch, J.; Schirmer, T. *Structure* **1996**, *4*, 127.
(5) Cowan, J. A. *Chem. Rev.* **1998**, *98*, 1067.
(6) Gilman, A. G. *Annu. Rev. Biochem.* **1987**, *56*, 615.
(7) Berridge, M. J.; Irvine, R. F. *Nature* **1989**, *341*, 197.
(8) Harwood, A. J. *Cell* **2001**, *105*, 821.
(9) Gould, T. D.; Quiroz, J. A.; Singh, J.; Zarate, J. C. A.; Mnji, H. K. *Mol. Psychiatry* **2004**, *9*, 734.
(10) Dudev, T.; Cowan, J. A.; Lim, C. *J. Am. Chem. Soc.* **1999**, *121*, 7665.
(11) Dudev, T.; Lim, C. *Chem. Rev.* **2003**, *103*, 773.
(12) Yang, T.-Y.; Dudev, T.; Lim, C. *J. Am. Chem. Soc.* **2008**, *130*, 3844.
(13) Berman, H. M.; et al. *Acta Crystallogr. D* **2002**, *58*, 899.
(14) Black, C. B.; Cowan, J. A. *J. Am. Chem. Soc.* **1994**, *116*, 1174.
(15) Dudev, T.; Lim, C. *J. Phys. Chem. B* **2004**, *108*, 4546.
(16) Dudev, T.; Lim, C. *Acc. Chem. Res.* **2007**, *40*, 85–93.
(17) Dudev, T.; Lin, Y. L.; Dudev, M.; Lim, C. *J. Am. Chem. Soc.* **2003**, *125*, 3168.
(18) Dudev, T.; Lim, C. *J. Phys. Chem. B* **2001**, *105*, 4446.
(19) Babu, C. S.; Dudev, T.; Casareno, R.; Cowan, J. A.; Lim, C. *J. Am. Chem. Soc.* **2003**, *125*, 9318.
(20) Dudev, T.; Lim, C. *Annu. Rev. Biophys.* **2008**, *37*, 97.
(21) Dudev, T.; Lim, C. *J. Am. Chem. Soc.* **2009**, *113*, 11754.
(22) Pontikis, G.; Borden, J.; Martinek, V.; Florian, J. *J. Phys. Chem. A* **2009**, *113*, 3588.

(23) Remko, M.; Fitz, D.; Rode, B. M. *Amino Acids* **2010**, *39*, 1309.
(24) Dudev, T.; Chang, L.-Y.; Lim, C. *J. Am. Chem. Soc.* **2005**, *127*, 4091.
(25) Rezabal, E.; Mercero, J. M.; Lopez, X.; Ugalde, J. M. *J. Inorg. Biochem.* **2006**, *100*, 374.
(26) Rezabal, E.; Mercero, J. M.; Lopez, X.; Ugalde, J. M. *J. Inorg. Biochem.* **2007**, *101*, 1192.
(27) Rezabal, E.; Mercero, J. M.; Lopez, X.; Ugalde, J. M. *ChemPhysChem* **2007**, *8*, 2119.
(28) Garmer, D. R.; Gresh, N. *J. Am. Chem. Soc.* **1994**, *116*, 3556.
(29) Dudev, T.; Lim, C. *J. Phys. Chem. B* **2000**, *104*, 3692.
(30) Romani, A.; Scarpa, A. *Arch. Biochem. Biophys.* **1992**, *298*, 1.
(31) Niki, I.; Yokokura, H.; Sudo, T.; Kato, M.; Hidaka, H. *J. Biochem.* **1996**, *120*, 685.
(32) Suhy, D. A.; Simon, K. D.; Linzer, D. I. H.; O'Halloran, T. V. *J. Biol. Chem.* **1999**, *274*, 9183.
(33) MacDonald, T. L.; Martin, R. B. *Trends Biochem. Sci.* **1988**, *13*, 15.
(34) Collery, P.; Pirer, L.; Manfait, M.; Etienne, J. E. *Alzheimer's disease and dimentia syndromes consecutive to imbalanced mineral methabolisms subsequent to blood brain barrier alteration*; John Libbey-Eurotext: London-Paris, 1990.
(35) Marmol, F. *Progr. Neuro-Psychopharmacol. Biol. Psychiatry* **2008**, *32*, 1761.
(36) Shannon, R. D. *Acta Crystallogr. A* **1976**, *32*, 751.
(37) Friedman, H. L.; Krishnan, C. V. In *Water: A comprehensive treatise*; Franks, F., Ed.; Plenum Press: New York, 1973; Vol. 3, p 1.
(38) Srinivasan, C.; Toon, J.; Amari, L.; Abukhdeir, A. M.; Hamm, H.; Geraldes, C. G. C.; Ho, Y.-K.; de Freitas, D. M. *J. Inorg. Biochem.* **2004**, *98*, 691.
(39) Ryves, W. J.; Harwood, A. J. *Biochem. Biophys. Res. Commun.* **2001**, *280*, 720.
(40) Ryves, W. J.; Dajani, R.; Pearl, L.; Harwood, A. J. *Biochem. Biophys. Res. Commun.* **2002**, *290*, 967.
(41) Leech, A. P.; Baker, G. R.; Shute, J. K.; Cohen, M. A.; Gani, D. *Eur. J. Biochem.* **1993**, *212*, 693.
(42) Inhorn, R. C.; Majerus, P. W. *J. Biol. Chem.* **1987**, *262*, 15946.
(43) Villeret, H. S.; Fromm, H. J.; Lipscomb, W. N. *Proc. Natl. Acad. Sci. U.S.A.* **1995**, *92*, 8916.
(44) de Freitas, D. M.; Amari, L.; Srinivasan, C.; Rong, Q.; Ramasamy, R.; Abraha, A.; Geraldes, C. F. G. C.; Boyd, M. K. *Biochemistry* **1994**, *33*, 4101.
(45) Jernigan, R.; Raghunathan, G.; Bahar, I. *Curr. Opin. Struct. Biol.* **1994**, *4*, 256.
(46) Marcus, Y. *Chem Rev* **1988**, *88*, 1475.
(47) Dudev, M.; Wang, J.; Dudev, T.; Lim, C. *J. Phys. Chem. B* **2006**, *110*, 1889.
(48) Tunell, I.; Lim, C. *Inorg. Chem.* **2006**, *45*, 4811–4819.
(49) Frisch, M. J. et al. *Gaussian 03*; Gaussian, Inc.: Pittsburgh, PA, 2003.
(50) Dudev, T.; Lim, C. *J. Am. Chem. Soc.* **2009**, *131*, 8092.
(51) McQuarrie, D. A. *Statistical Mechanics*; Harper and Row: New York, 1976.
(52) Wong, M. W. *Chem. Phys. Lett.* **1996**, *256*, 391.
(53) Gilson, M. K.; Honig, B. H. *J. Comput. Chem.* **1988**, *9*, 327.
(54) Chan, S. L.; Lim, C. *J. Phys. Chem.* **1994**, *98*, 692.
(55) Bashford, D. In *Scientific Computing in Object-Oriented Parallel Environments*; Ishikawa, Y., Oldehoeft, R. R., Reynders, V. W., Tholburn, M., Eds.; Springer: Berlin, 1997; Vol. 1343, p 233.
(56) Dudev, T.; Lim, C. *J. Am. Chem. Soc.* **2006**, *128*, 1553.
(57) Brooks, B. R.; Bruccoleri, R. E.; Olafson, B. D.; States, D. J.; Swaminathan, S.; Karplus, M. *J. Comput. Chem.* **1983**, *4*, 187.
(58) Smith, R. M.; Martell, A. E. *Sci. Total Environ.* **1987**, *64*, 125.
(59) Jope, R. S. *Trends Pharmacol. Sci.* **2003**, *24*, 441.
(60) Kozikowski, A. P.; Gaisina, I. N.; Yuan, H.; Petukhov, P. A.; Blond, S. Y.; Fedolak, A.; Caldarone, B.; McGonigle, P. *J. Am. Chem. Soc.* **2007**, *129*, 8328.
(61) Aoki, M.; Yokota, T.; Sugiura, I.; Sasaki, C.; Hasegawa, T.; Okumura, C.; Ishiguro, K.; Kohno, T.; Sugio, S.; Matsuzaki, T. *Acta Crystallogr.* **2004**, *D60*, 439.
(62) Bertrand, J. A.; Thieffine, S.; Vulpetti, A.; Cristiani, C.; Valsasina, B.; Knapp, S.; Kalisz, H. M.; Flocco, M. *J. Mol. Biol.* **2003**, *333*, 393.
(63) Bone, R.; Frank, L.; Springer, J. P.; Atack, J. R. *Biochemistry* **1994**, *33*, 9468.
(64) Johnson, K. A.; Chen, L.; Yang, H.; Roberts, M. F.; Stec, B. *Biochemistry* **2001**, *40*, 618.
(65) Gill, R.; Mohammed, F.; Badyal, R.; Coates, L.; Erskine, P.; Thompson, D.; Cooper, J.; Gore, M.; Wood, S. *Acta Crystallogr.* **2005**, *D61*, 545.
(66) Li, Z.; Stieglitz, K. A.; Shrout, A. L.; Wei, Y.; Weis, R. M.; Stec, B.; Roberts, M. F. *Protein Sci.* **2010**, *19*, 309.
(67) Patel, S.; Martinez-Ripoll, M.; Blundell, T. L.; Albert, A. *J. Mol. Biol.* **2002**, *320*, 1087.
(68) Lu, S.-Y.; Jiang, Y.-J.; Zou, J.-W.; Wu, T.-X. *Phys. Chem. Chem. Phys.* **2011**, *13*, 7014.
(69) Sun, H.; Jiang, Y.-J.; Yu, Q.-S.; Luo, C.-C.; Zou, J.-W. *J. Mol. Model.* **2011**, *17*, 377.
(70) Pollack, S. J.; Knowles, M. R.; Atack, J. R.; Broughton, H. B.; Ragan, C. I.; Osborne, S.; McAllister, G. *Eur. J. Biochem.* **1993**, *217*, 281.
(71) Pollack, S. J.; Atack, J. R.; Knowles, M. R.; McAllister, G.; Ragan, C. I.; Baker, R.; Fletcher, S. R.; Iversen, L. L.; Broughton, H. B. *Proc. Natl. Acad. Sci. U.S.A.* **1994**, *91*, 5766.